ISSN No: 2348-4845
International Journal & Magazine of Engineering, Technology, Management and Research
A Peer Reviewed Open Access International Journal

Implementation of Model Reference Adaptive Controller by RCC Technique for Renewable Energy System

M.P.Reena
M.Tech (Power Electronics),
Department of Electrical Engineering,
Swami Ramananda Tirtha Institute of Science & Technology, Nalgonda, T.S, India.

B.Srinu
Assistant professor
Department of Electrical Engineering,
Swami Ramananda Tirtha Institute of Science & Technology, Nalgonda, T.S, India.

Abstract:

This paper proposes a two-layer adaptive control architecture that can effectively handle the uncertainties and perturbations in the photovoltaic systems and the environment. The first layer of control is ripple correlation control (RCC), and the second layer is model reference adaptive control (MRAC). Photovoltaic systems provide promising ways to generate clean electric power. MPPT technologies have been used in photovoltaic systems to deliver the maximum power output to the load under changes of solar insolation and solar panel's temperature. The performance of the proposed technique was observed by MATLAB/simulink software.

Index terms:

Maximum power point tracking, solar energy conversion system, MRAC, RCC.

I.INTRODUCTION:

Photovoltaic system is a critical component to achieve the solar energy through an environmentally-friendly and efficient way. Maximum power point tracking algorithm (MPPT) keeps the photovoltaic systems continuously delivering the maximum power output to the utility, regardless of the variation in environment condition. Under the effect of MPPT algorithm, the photovoltaic systems are capable of adapting itself to the environment change and delivering the maximum power output.

Generally, the MPPT controller is embedded in the power electronic converter systems, so that the corresponding optimal duty cycle is updated to the photovoltaic power conversion system to generate the maximum power point output.A series of the control algorithms for the MPPT are well understood at the present time, due to the significance of improving the photovoltaic systems performance efficiency. The underlying principle of maximum power point tracking algorithm is to use the ripple voltage or current component to identify the variation trend of the power output with the knowledge of the current versus voltage and the power output versus the voltage of the PV system.

Generally, the operating point for different environment conditions varies and the characteristics of the I-V and P-V are generally illustrated in the way shown in Figure 1. The corresponding voltage array for the maximum power point is varied, as a result of the variation in the solar insolation and the panel temperatures. By implementing the photovoltaic system with a DC-DC converter integrated with an MPPT controller, the nominal voltage can be modulated so that the maximum power is delivered. To track the maximum power point with dynamic changes, many algorithms deliver appropriate solutions in literature to solve the problem.

Many refined MPPT algorithms have been optimizing the digital realization, implementation complexity and operating cost since 1970s. Among these algorithms, ripple correlation control (RCC) is a better solution to solve the MPPT problem, considering the issue of stability, complexity and expense.

ISSN No: 2348-4845
International Journal & Magazine of Engineering, Technology, Management and Research
A Peer Reviewed Open Access International Journal

Ripple correlation control is utilizing the integration of the correlation between the ripple power component and the ripple current or voltage component in the power electronic systems to obtain the duty cycle of the optimal power output.The other control algorithm is model reference adaptive control (MRAC). It is designed to compensate for changing the undesired characteristic of the photovoltaic power conversion system. As a result, the performance of the power output is improved. MRAC has been analyzed since 1968 and has already been a widely-used technology in the modern control engineering and many other fields. MRAC is one of the robust prevalent control approaches in the adaptive control branch because MRAC is expertise in tuning the system's performance to the nominal characteristic when the system's parameter is unknown at prior.

In this project, under the effect of environment conditions, the specific dynamics of the power conversion system, or equivalently, the transfer function of the plant, is a nonlinear system. In each specific working environment, an equivalent transfer function between the duty cycle and the voltage array output can be uniquely determined. Therefore, the MRAC algorithm is a suitable solution to alter the characteristics of the plant, considering the unknown parameters of the single-input single-output plant (SISO). In the MRAC algorithm, given a nominal reference model for photovoltaic system, through constantly tuning the parameters of the controller, the characteristics of the plant will converge to the characteristics of the reference model, meanwhile, the deviation between the reference model and plant model output will approach to zero, gradually.

II.STRUCTURE OF ENTIRE SYSTEM:

In the last section, the two-layer structure of the control system is briefly discussed, as shown in Figure 2. By mean of the MPPT controller, equivalently RCC algorithm, the duty cycle is fed into the switching transistor of the converter; hence the maximum power output can be found. Then through the MRAC component, the transfer function of the converter is adapted. After the adaptation, the maximum power output will be delivered to the utility. In this project, it is required to obtain the model of the converter, as shown in Figure 2, which describes the relationship between the dynamics of duty cycle and the voltage output.

When the duty cycle is updated, following by the environment change, the derivation of the voltage array in the solar panel will be updated as well. To get the transfer function of the actual plant, one can derive it through the equivalent small signal circuit of the photovoltaic power conversion system, as detailed shown in Figure 3 [1]:As shown in Figure 3, the resistor R1 is analog to the solar irradiance or temperature change with the small signal of the voltage, vPV˜, to the small signal of the current, iPV˜. When the solar insolation changes, the specific operating point of the PV power conversion system changes, as a result, the value of the resistor varied.

And hence the value of the resistor is unable to predict because it is extremely hard to predict the irradiance of the sun throughout a day. To obtain the characteristic of the nonlinear system, linearization at a certain operating point of solar intensity is required. And Figure 3 is the linearization process of the nonlinear system. As shown in the following, one can express the small signal equivalent circuit of the system in this way.

$$\frac{\tilde{v}_{PV}}{R_I} + s\tilde{v}_{PV}C_I = \frac{\dot{q}(D)\tilde{d} - \tilde{v}_{PV}}{sL_O}$$

wherevPV˜ is the voltage input difference, corresponding to the solar insolation change. The resistor R1 is an equivalent representation of the current. The voltage over the booster converter is q(D), as a function of the DC component of the duty cycle, and the q(D) can be expressed as:

q (D) = = (1-D) Vo ----q (D) = -Vo.

If the relationship between the array voltage changes to the duty cycle change is GVP(s), then GVP(s) can be expressed as follow:

$$G_{VP}(s) = \frac{\tilde{v}_{PV}}{\tilde{d}} = \frac{\dot{q}(D)}{L_O C_I s^2 + \frac{L_O}{R_I}s + 1}$$

Re-arranged into the following form and it is second order system

$$G_{sec}(s) = \frac{\mu\omega_n{}^2}{s^2 + 2\xi\omega_n s + \omega_n{}^2}$$

$$G_{VP}(s) = \frac{\frac{-V_O}{L_O C_I}}{s^2 + \frac{1}{C_I R_I}s + \frac{1}{L_O C_I}}$$

ISSN No: 2348-4845
International Journal & Magazine of Engineering, Technology, Management and Research
A Peer Reviewed Open Access International Journal

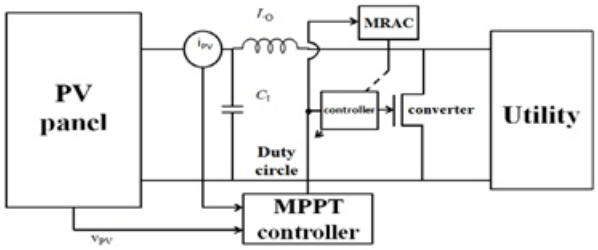

Fig 2: The scheme of entire control system.

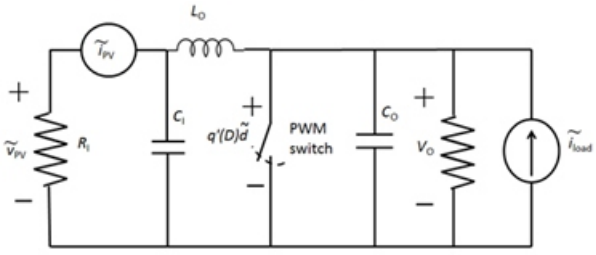

Figure 3: The equivalent small signal circuit of converter.

This transfer function is derived from a linearization of a second non-linear system, seem in the Figure 3. The value of the capacitor and inductor are fixed. However, the external solar insolation changing constantly, as a result, different P-V curve would lead to the maximum power point at different region on that curve figures, which can be explicitly shown in the Figure 1.

Similarly, varying environment condition will lead to varying value of the resistor, , and it is hard to acquire the specific value of the resistor when the operating point of the system continuously changing. As a result, the damping ratio varies with the specific value of resistor and the step response of the voltage output with different equivalent value of resistor can be seen in the Figure 4:

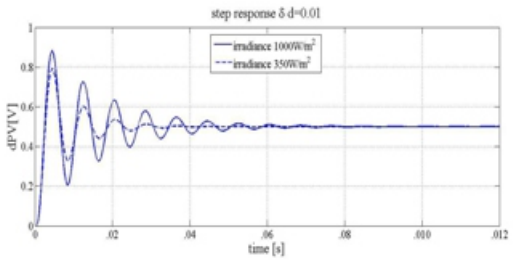

Figure 4: The step response of the under-damped converter.

In Figure 4, the voltage response shows the oscillation with different damping ratio and changing dc gain.

With the effect of external irradiance change, such oscillation in the transient period inevitable occurs and the various time constant for each distinct system which corresponds to the sunshine intensity, will significantly extend the converging rate of the converter and in the most time the system cannot deliver the maximum power output. Besides, there is no straightforward approach to estimate the parameters in the transfer function of the plant to change the characteristics of the plant and eliminate oscillation during the transient period.

DESIGN ANALYSIS FOR MRAC AND RCC:
Scheme of the MRAC and proof of stability:

As discussed in Section 2 that the transfer function between the duty cycle and the voltage output in the array is an under-damped second order system. When the updated duty cycle inputs into dynamic system, the voltage output will display decaying oscillation in the transient period and gradually converge to the nominal voltage of the maximum power point. It is desired that the transfer function has the critically-damped characteristic, not only because the time constant will be minimized compared to the time constant of the under-damped system, but also no oscillation will occur in the transient response. To obtain a critically damped response for the given transfer function, the general MRAC architecture is shown in the Figure 5.

The input to the overall system, r is the duty cycle obtained in the ripple correlation control method. The specific transfer function of the plant model, or equivalently the system of photovoltaic power conversion, can be obtained in the following section. Also, it is certainly that the transfer function of the plant model is a second order system and the relative degree of the system is two. The fundamental object of MRAC used in this project is to draw the characteristic of the plant to the characteristics of the reference model. By designing an ideal reference model, after adaptation, the plant model will have such characteristics as well. The error signal as well as the input and the output of the plant, adaptively enable the adjustment parameters to tune the controller so that the parameters of the plant will converge to the parameters of the reference model.

ISSN No: 2348-4845
International Journal & Magazine of Engineering, Technology, Management and Research
A Peer Reviewed Open Access International Journal

Eventually, the error between the plant and the reference model will drive to zero and the controller parameters will converge to the nominal controller parameters, so that the full convergence is achieved and thus the adapted array voltage tracks the theoretical MPP voltage.

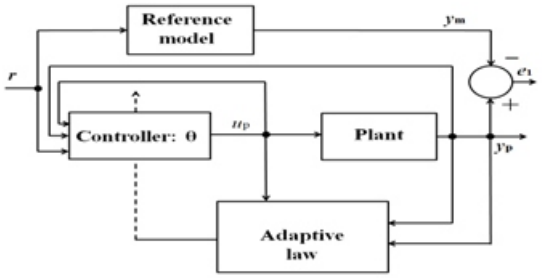

Figure 5: The general scheme of the MRAC structure.

Generally, for any signal, u(t) is considered as persistently exciting if the following condition is satisfied:

$$\int_{t}^{t+T_0} u^2(\tau)d\tau \geq \alpha_0 T_0 \qquad \text{- 3.1}$$

For any positive value t, there exists α0 and To to meet the condition, then the signal u(t) satisfies the PE condition. It is also necessary to interpret that the input signal should be 2n order with a given nth order plant model. In the simulation, it is instructive to know that the combination of step function and sin function are all satisfied with the PE condition.In the general MRAC architecture, quite many different methods can be utilized to find the adaptive laws for the controller to make sure the error signal converge. Basically, the prevalent method at the present is using Lyapunov function to ensure the system converge asymptotically. There are several definitions to determine the meaning of stability in the control theory. The stability in the sense of Lyapunov is a mild approach to find the adaptive law by ensuring the asymptotic stability. An arbitrary point is stable if for any >0, there always exists a value >0, so that the norm value between the current point and the nominal equilibrium point is always less than the. In other word, the stability in the sense of Lyapunov is independent of the initial condition of the system and is significantly sufficient to guarantee the stability. As shown in Section 2, the relative degree plant of the photovoltaic power conversion system e.g. (deg(Dm)-deg(Nm)) is two. The transfer functions for the reference model is Gvm(s) and the plant model is GVP(s).

$$G_{vm}(s) = \frac{y_m}{r} = k_m \frac{1}{s^2 + a_m s + b_m} = k_m \frac{N_m(s)}{D_m(s)}$$

$$G_{vp}(s) = \frac{y_p}{u_p} = k_p \frac{1}{s^2 + a_p s + b_p} = k_p \frac{N_p(s)}{D_p(s)} \qquad \text{- 3.2}$$

Where km and kp are the chosen gain of the systems, and am, bm¬, ap and bo are the chosen parameters of the reference model and the plant model. A critical damping system can be obtained under the condition being satisfied: am=2√bm. Several assumptions about should be announced before the further analysis:

- The reference model is controllable and observable
- The degree of denominator of plant and the sign of the gain is known.
- Both the reference model and the plant model are controllable and observable

The expression for the controller is the combination of the input, output of the plant and the input of the reference model.

$$u_p = \theta_1 \frac{\alpha(s)}{\Lambda(s)} u_p + \theta_2 \frac{\alpha(s)}{\Lambda(s)} y_p + \theta_3 y_p + c_0 r = \vec{\theta}\vec{\omega} \qquad \text{- 3.3}$$

u_p is the input to the plant, vector $\theta' = [\theta_1, \theta_2, \theta_3, c_0]$ is the parameter vector of the controller, which is updated through the adaptive law which is required to find. Furthermore, r and y_p are the input to the system and the output of the plant, respectively, while $\alpha(s)/\Lambda(s)$ is a arbitrarily designed nth ($deg(D_m)$-1) order stable filter as denoted in Figure 6.

The filter is used to ensure the stability of the system through derivative operation in the high-order system. Actually, in the practical situations, the only available variables to be measured are the the input of the system, the output of the reference model and of the plant. Therefore, other forms of intermediate variables, such as high order differentiation of the output is hard to measure and the derivation operating will lead the system to be unstable and is unobservable.

The polynomial Λ(s) contains the polynomial $N_m(s)$, the numerator of the transfer function for the reference model, and the expression of the polynomial is:

$\Lambda(s) = \Lambda_o(s)\, N_m(s)$.

In the state variable vector $w' = [w_1, w_2, y_p, r]$ variable w_1 is equal to $[\alpha(s)/\Lambda(s)]u_p$ and variable $w_2$is equal to $[\alpha(s)/\Lambda(s)]y_p$. To obtain the controller's parameter and converge the plant model to the reference model, one can substitute r for u_p, according to the

ISSN No: 2348-4845
International Journal & Magazine of Engineering, Technology, Management and Research
A Peer Reviewed Open Access International Journal

relationship in (3-3). Then the transfers function between the input of the system, r and the output of the plant y_p...

$$\frac{y_p}{r}=\frac{k_p N_p(s)\Lambda(s)c_0}{D_p(s)\left(\Lambda(s)-\theta_1\alpha(s)\right)-\theta_2 k_p N_p(s)\alpha(s)-\theta_3\Lambda(s)k_p N_p(s)} \quad -3.4$$

One crucial difficulty lying in this work is the unknown parameter of the power converter due to that changing resistor in the circuit, shown in Figure 3. Therefore, a reasonable approach to overcome the obstacle is using on-line estimation of the controller parameter to represent the nominal controller parameter.

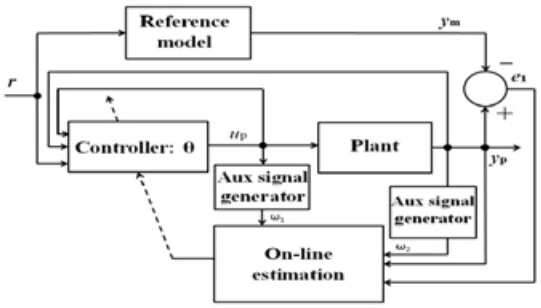

Figure 6: The proposed MRAC in MPPT.

As shown in Figure 6, the input and the output of the plant model are fed into the observer, so that the auxiliary signal w1 and w2 are joined into the on-line estimation to tuning the controller parameters. Therefore, several consequence need to be noticed: firstly, the parameter vector of the controller will be changed into the estimation parameter vector, *'. Secondly, with the realization of the adaptive observers in this system, the following properties can be guaranteed with the PE conditioned input:

- All the signals in the system are uniformly bounded
- The error between the actual output of the plant model and the estimated output of the plant model will approach to zero as time goes to infinity
- The error between the state space realization of the plant model and the estimated realization will converge to zero exponentially fast as time goes infinity.

By iteratively using the output of the reference model and the plant, the controller parameters converge to the nominal parameters. Thus, the form of in (3.3) can be expressed as seen in (3.5):

$$u_p = \overrightarrow{\theta^*}\overrightarrow{\omega} \quad -3.5$$

Arbitrarily choosing $\Lambda(s) = 1+s$ and hence $w_1 = [\alpha(s)/\Lambda(s)] = 1/(1+s)$ and $w_2 = [\alpha(s)/\Lambda(s)]y_p = 1/(1+s)y_p$. These two state observers' equations can be represented as shown in (4-7):

$$\begin{aligned}\dot{\omega}_1 &= \omega_1 + u_p, \qquad \omega_1(0) = 0\\ \dot{\omega}_2 &= \omega_2 + y_p, \qquad \omega_2(0) = 0\end{aligned} \quad -3.6$$

The observers in (4.7) are implemented to estimate the minimal realization of the plant to obtain the error between the reference model output and the plant model output [13]. The state-space realization of the transfer function for the plant and reference model, shown in (3.2), can be decomposed into the state space equation, shown as follows:

$$\begin{aligned}G_{vm}(s) &= \frac{y_m}{r} = C_m(sI - A_m)^{-1}B_m\\ G_{vp}(s) &= \frac{y_p}{u_n} = C_p(sI - A_p)^{-1}B_p\end{aligned} \quad -3.7$$

By substituting the input of the plant mode, up, with the controller expression, the state space of the plant model in (3.8) can be obtained:The polynomial in the-second equation of (3.5) is the determinant of matrix A1. The roots of this polynomial are located in the left-hand side of the s-plane, according to the three roots, of the right hand side of the equation, are located in the left-hand side of the s-plane in (3.5). Therefore, it can be inferred that these two systems are stable. By subtracting the reference model's state space equation from the plant's state space equation, the state-space equations for the controller parameter's error and the tracking error are obtained as follows:Where e = X0-X1 is the state error, e1 = yp -ym is the tracking error signal of the plant, and T' = T - T'*is the controller parameter's error between the nominal parameter and the actual parameter of the controller. The overall transfer function of the tracking error signal and the controller parameters error can be obtained as follows:

$$e_1 = C_1^T(sI - A_1)^{-1}B_1\tilde{\theta}^T\omega = G_{vm}(s)\frac{1}{c^0}\tilde{\theta}^T\omega \quad -3.8$$

In term of stability, a Lyapunov-like function is to obtain suitable adaptive law for the controller's expression. Applying an identity polynomial: (s+g)(s+g)-1 (term s+g needs to be stable) to both sides of (3.12) to decrease the relative degree of the overall transfer function, (3.14) is derived from (3.12):

ISSN No: 2348-4845
International Journal & Magazine of Engineering, Technology, Management and Research
A Peer Reviewed Open Access International Journal

Where several new state variables are introduced: uq= [1/(s+g)]up, φ=[1/(s+g)w]1/(s+g)(w1, w2, yp, r). The term s+g will be absorbed into the matrix B1. Since uq =Tφ, equivalently, the controller's input can be updated as:

$$u_p = \theta^T \omega + \dot{\theta}^T \phi \qquad -3.9$$

According to the derivations above, the overall MRAC adaptive rules can be concluded as follows and each item in (3.16) is the function with zero value initial conditions:A series of adaptive control updating laws are obtained with the entire scheme of MRAC found, two important conceptions are instructive to be informed: firstly, signal in the closed-loop plant is bounded and the tracking error signal will converge to zero asymptotically. Secondly, if the numerator and the denominator of the plant is co-prime and the input signal is sufficiently rich of order, the tracking error signal will converge exponentially fast.

RIPPLE CORRELATION CONTROL:

To deliver the maximum power output to the load at the steady state, RCC algorithm is utilized to calculate the duty cycle. RCC algorithm was recently developed and reported, where it was shown that the switching transistor will result in an inherent ripple voltage or current component, which can be utilized to track the location of the maximum power point.

RCC algorithm is an improved algorithm based on the P&O method, because it avoids external energy to generate the voltage ripple for tracking the MPP.

In additional, it is proven in the report that RCC algorithm is asymptotically convergence to the MPP. As shown in the Figure 1, there is only one peak power value in the PV curve or the PI curve, where the maximum power delivery is obtained. Correlating the derivation of the power output and the derivation of the voltage output, the correlation identifies whether the present voltage is lower or higher than the nominal voltage output.

To mitigate the array capacitance in the circuit, it is desired to use the ripple voltage component in the correlation, as the following formula to calculate the duty cycle shown:

$$\begin{aligned} &\tilde{p}_{PV}\tilde{v}_{PV} > 0 \ \text{ when } V_{PV} < V_L^* \\ &\tilde{p}_{PV}\tilde{v}_{PV} < 0 \ \text{ when } V_{PV} < V_L^* \\ &\tilde{p}_{PV}\tilde{v}_{PV} = 0 \ \text{ when } V_{PV} = V_L^* \end{aligned} \qquad -3.11$$

The control law can be seen as:

$$d = k \int \tilde{p}_{PV}\tilde{v}_{PV}\, dt \qquad -3.12$$

Where p_{PV}'and v_{PV}' are the ripple component of the array power and voltage, and k is the negative valued gain. It can be described as follows: if v_{PV} increases and it result an increasing p_{PV}, the system's operating point is located on the left side of the MPP, therefore the value of d is decreasing; similarly, if vPV increases and it result a decreasing pPV, the system's operating point is located on the right side of the MPP. Inspecting, the maximum power point can be obtained when the derivation of d is equal to zero because that is the place where the voltage array is equal to the nominal one and the change of d can be assumed to zero.

Given the mathematically proof for the stability of the RCC algorithm, the corresponding duty cycle for the maximum power point under various solar insolations can be achieved. In the RCC algorithm, the underlying principle is using whatever ripple is already presented in the system to determine the location of the maximum power point.

Alternatively, the control algorithm by mean of the ripple current component can be realized as well because the P-I curve and P-V curve are similar to each other. One modification is the sign of the gain value of k needs to be reversed. However, due to the practical implementation, the issue of the parasite capacitor is necessary to be considered, the voltage ripple component is obviously advantageous than the current ripple component.

As inferred from the literature review in Section 1, many improved and alternative version of RCC algorithms have been developed to replace the original one, another way to propose the RCC algorithm is using the direct integrand of the ratio between the power output and the ripple component of the voltage or the power output and the ripple component of the current:

$$d = \int \frac{dp}{dv_L}\, dt \qquad -3.12$$

ISSN No: 2348-4845
International Journal & Magazine of Engineering, Technology, Management and Research
A Peer Reviewed Open Access International Journal

The control law in is hard to expect working due to the complexity of realizing the integrand of this ratio in the circuit. Moreover, like the drawback of P&O MPPT algorithm, the ratio of signal-to-noise is unavailable and hence this is not sufficient to make the judgment that the duty cycle for the maximum pwer point is achieved because the ratio between the ripple power and voltage component is impossible to maintain ideally being zero for quite amount of time. Due to the effect of noise, this control law is not reliable to make the determination.With increasing focus on the simple implementation of the algorithm in circuit, one useful control law makes use of the sign function to track the MPP in the circuit. As shown the control law is:

$$d = k \int sgn\left(\frac{di_L}{dt}\right) sgn\left(\frac{dp}{dt}\right) dt \qquad -3.13$$

The effect of noise is mitigated because of the sign function only focus on whether the derivation of d is larger, smaller or equal to zero. And this control law is easy to realize in electronics hardware by using logic circuit at an inexpensive cost. This control law was also proved mathematically that it is stable, and thus it is an alternative RCC algorithm to be used in this project.

STEP-UP (BOOST) CONVERTER

Figure 7(a) depicts a step-up or a PWM boost converter. It is comprised of dc input voltage source VS , boost inductor L, controlled switch S, diode D, filter capacitor C, and load resistance R. The converter waveforms in the CCM are presented in Fig. 7(b). When the switch S is in the on state, current in the boost inductor increases linearly. The diode D is off at the time. When the switch S is turned off, the energy stored in the inductor is released through the diode to the input RC circuit.

Using the Faraday's law for the boost inductor.

VSDT = (VO – VS) (1 – D)T

From which the dc voltage transfer function turns out to be

MV VO/VS = 1/1 – D

As the name of the converter suggests, the output voltage is always greater than the input voltage.

The boost converter operates in the CCM for L > Lb where

Lb = (1 – D)2DR /2f

For D = 0.5, R = 10 ohm, and f = 100 kHz, the boundary value of the inductance is Lb = 6.25µH.

As shown in Fig. 7(b), the current supplied to the output RC circuit is discontinuous. Thus, a larger filter capacitor is required in comparison to that in the buck-derived converters to limit the output voltage ripple.

The filter capacitor must provide the output dc current to the load when the diode D is off. The minimum value of the filter capacitance that results in the voltage ripple Vr is given by

Cmin = DVO/VrRf

At D = 0.5, Vr /VO = 1%, R = 10 ohm, and f = 100 kHz, the minimum capacitance for the boost converter is Cmin = 50µF. The boost converter does not have a popular transformer (isolated) version.

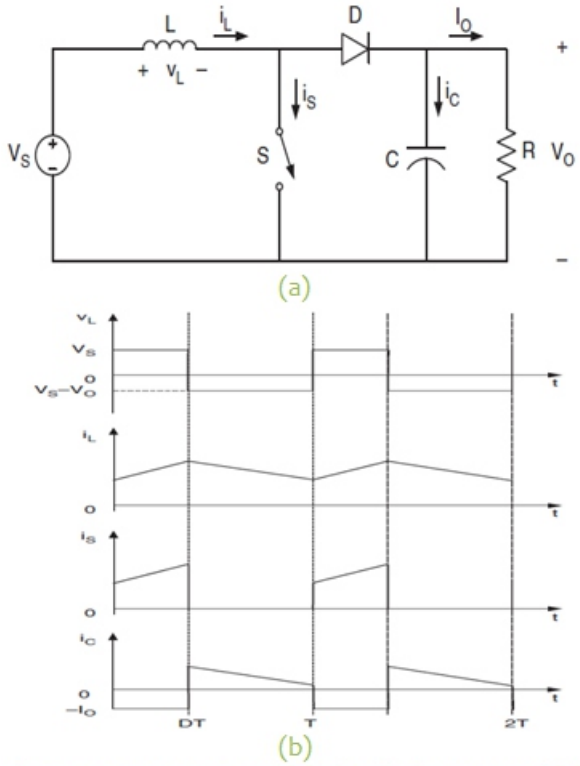

Fig 7: Boost converters: (a) circuit diagram and (b) waveforms.

SIMULATION RESULTS:

The adaptive controller presented in Section III was then simulated for verification. The plant model was chosen to deliver an actual array voltage with an underdamped step response. The reference model was designed to deliver a theoretical MPP voltage with a critically damped step response. Its damping ratio, which equals am/2√bm, is the determining factor as inferred from. Normally, the ratio is chosen to be either exactly 1 or slightly less than 1. In the latter case, the step response rises faster at the cost of slight overshoot. The desired outcome of simulation would be that after the plant has undergone the adaptation phase, the parameters of the controlled plant would converge to the parameters of the reference model and thus the adapted array voltage would show critically damped behavior.

ISSN No: 2348-4845
International Journal & Magazine of Engineering, Technology, Management and Research
A Peer Reviewed Open Access International Journal

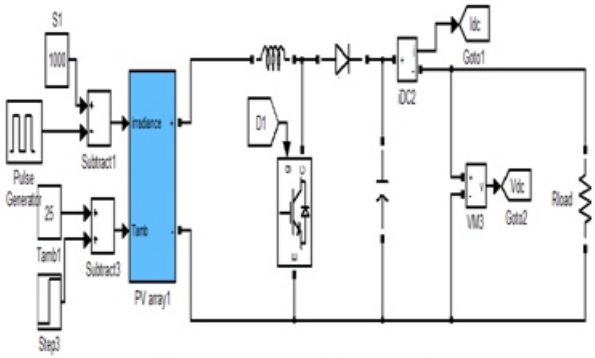

Fig 8: simulation design of proposed converter

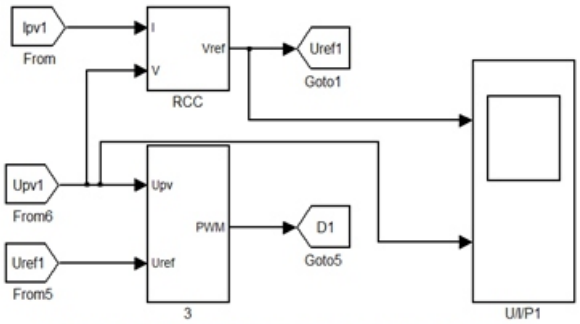

Fig 9: Model Reference Adaptive Control

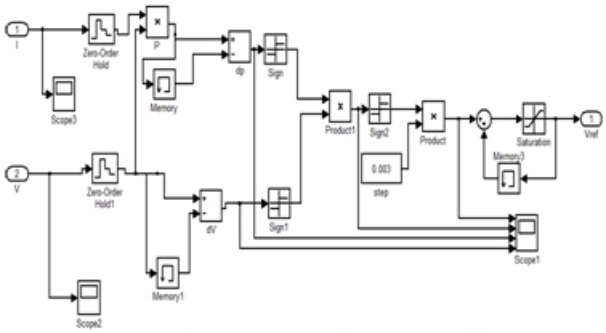

Fig 10: Ripple Co-relation Controller

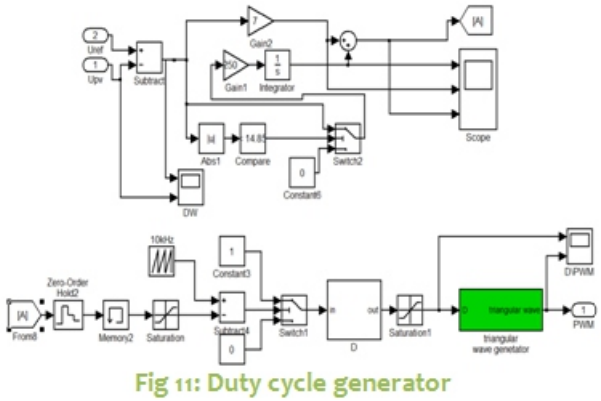

Fig 11: Duty cycle generator

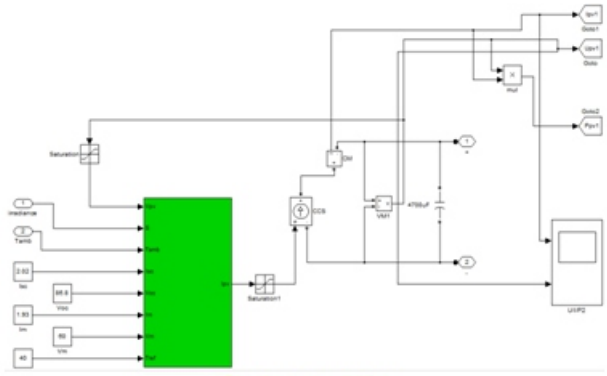

Fig 12: PV-Array

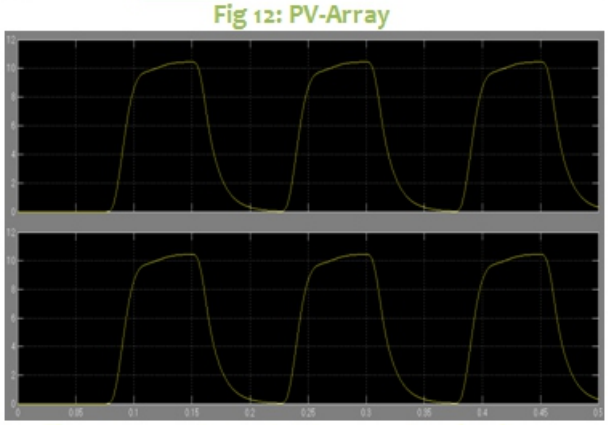

Fig 13: converter output current and voltage

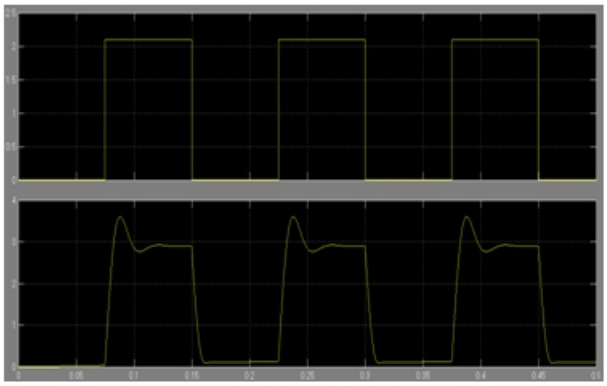

Fig 14: PV-array current and voltage

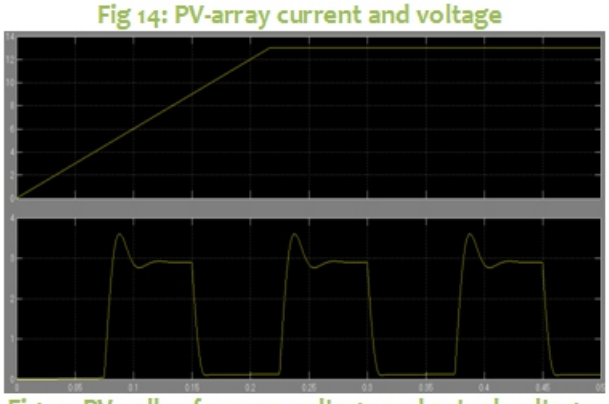

Fig 15: PV cell reference voltage and actual voltage

ISSN No: 2348-4845
International Journal & Magazine of Engineering, Technology, Management and Research
A Peer Reviewed Open Access International Journal

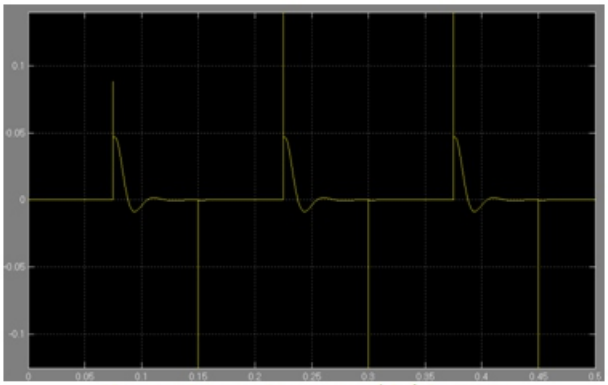

Fig 16: change in power (dp) in RCC

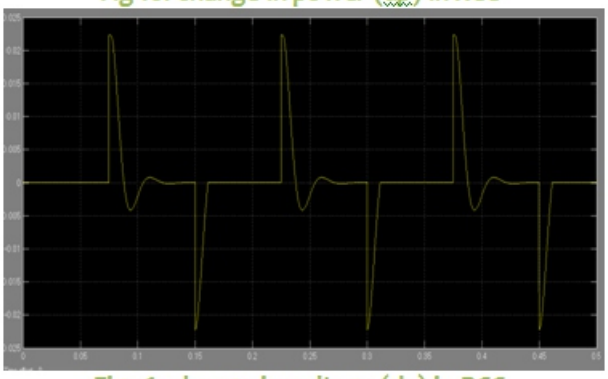

Fig 16: change in voltage (dv) in RCC

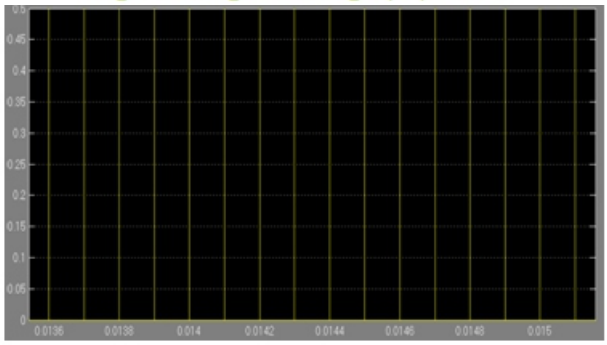

Fig 17: duty cycle

CONCLUSION:

The MPPT controllers are used to improve the power efficiency of the renewable energy systems. Critical issues to be considered in the MPPT algorithms include system complexity, uncertainty, and dynamical performance. Model Reference Adaptive Control for the generation of duty cycles for boost converter. The MRAC is designed with two-layer structure; they are having Ripple Co-relation control and duty cycle generator. This paper focused mostly on the design of the MRAC algorithm, which compensated the under-damped characteristics of the power conversion system. The characteristics given in simulation results are observed that proposed converter is having better performance.

REFERENCES:

[1] S. L. Brunton, C. W. Rowley, S. R.Kulkarni, and C. Clarkson, "Maximum power point tracking for photovoltaic optimization using ripple-based extremum seeking control," IEEE Trans. Power Electron., vol. 25, no. 10, pp. 2531–2540, Oct. 2010.

[2] R. A.Mastromauro,M. Liserre, T.Kerekes, and A. Dell'Aquila, "A single-phase voltage-controlled grid-connected photovoltaic system with power quality conditioner functionality," IEEE Trans. Ind. Electron., vol. 56, no. 11, pp. 4436–4444, Nov. 2009.

[3] A. K. Abdelsalam, A. M. Massoud, S. Ahmed, and P. N. Enjeti, "High-performance adaptive perturb and observe MPPT technique for photovoltaic-based microgrids," IEEE Trans. Power Electron., vol. 26, no. 4, pp. 1010–1021, Apr. 2011.

[4] M. A. Elgendy, B. Zahawi, and D. J. Atkinson, "Assessment of perturb and observe MPPT algorithm implementation techniques for PV pumping applications," IEEE Trans. Sustainable Energy, vol. 3, no. 1, pp. 21–33, Jan. 2012.

[5] G. Petrone, G. Spagnuolo, and M. Vitelli, "A multivariable perturb-and observe maximum power point tracking technique applied to a single-stage photovoltaic inverter," IEEE Trans. Ind. Electron., vol. 58, no. 1, pp. 76–84, Jan. 2011.

[6] S. Jain andV.Agarwal, "A new algorithm for rapid tracking of approximate maximum power point in photovoltaic systems," IEEE Power Electron. Lett., vol. 2, no. 1, pp. 16–19, Mar. 2004.

[7] N. Femia, G. Petrone, G. Spagnuolo, and M. Vitelli, "Optimization of perturb and observe maximum power point tracking method," IEEE Trans. Power Electron., vol. 20, no. 4, pp. 963–973, Jul. 2005.

[8] M. A. S. Masoum, H. Dehbonei, and E. F. Fuchs, "Theoretical and experimental analyses of photovoltaic systems with voltage and current-based maximum power-point tracking," IEEE Trans. Energy Convers., vol. 17, no. 4, pp. 514–522, Dec. 2002.

[9] T. Esram and P. L. Chapman, "Comparison of photovoltaic array maximum power point tracking techniques," IEEE Trans. Energy Convers., vol. 22, no. 2, pp. 439–449, Jun. 2007.

[10] M. Veerachary, T. Senjyu, and K. Uezato, "Neural-network-based maximum-power-point tracking of coupled-inductor interleaved-boost converter- supplied PV system using fuzzy controller," IEEE Trans. Ind. Electron., vol. 50, no. 4, pp. 749–758, Aug. 2003.